Experimental Evidence of Zonal Flows using HIBP Data

P.M. Schoch
Rensselaer Polytechnic Institute
Troy, NY 12180

Abstract:

Fluctuations of potential due to zonal flows have been previously reported but not correctly identified. Zonal flows can limit driftwave turbulence by shear decorrelation and may be the mechanism limiting transport in present experiments. Fluctuations of potential measured using the Heavy Ion Beam Probe (HIBP) on the Texas EXperimental Tokamak (TEXT) are shown to be the result of m=0 radial electric field fluctuations with a weak linear coupling to density fluctuation and a significant non-linear coupling to the driftwave fluctuations, consistent with zonal flows.

Resent publications have noted the likely importance of zonal flows as a mechanism to control turbulence levels in magnetically confined plasma.[1,2,3] Zonal flows have been numerically simulated.[4,5] Experimental evidence has been presented, for example from Langmuir probe measurements on H-1[6], both Phase Contrast and BES measurements on DIII-D[7,8] and by looking for three-wave coupling[9,10]. This paper presents experimental evidence in fusion relevant plasma over the plasma minor radius (unlike the H-1 results) and uses direct measurements of potential, unlike other results. The data presented was collected using a Heavy Ion Beam Probe, HIBP[11], on the Texas EXperimental Tokamak, TEXT[12]. The HIBP measures fluctuations of potential and it is shown that these fluctuations are due to zonal flow E_r fluctuations.

Quoting from Diamond et al[1] "Zonal flows are poloidally and toroidally symmetric ($k_\theta = k_z = 0$), zero frequency vortex modes with finite radial scale (k_r finite),…". The data presented show radial electric fields with these properties except the frequency is that of the Geodesic Acoustic Mode (GAM) and not zero Hz. The diagnostic was not optimized to measure zero frequency modes, (zero average frequency but finite frequency width,) but was sufficiently sensitive to state that zero frequency fluctuations are at least an order of magnitude weaker than those at the GAM frequency. Strong GAM electric field fluctuations were predicted as early as 1968 by Winson, Johnson and Dawson.[13] Their article suggests that the GAM may have been detected in the Model C Stellarator, though the strongest fluctuation detected has been identified as a resistive ballooning mode.[14,15] The GAM mode may be driven by damping of the zero frequency mode[1] (which in turn is driven by the Reynolds stress,) or may be directly driven by the interaction of the

pressure inhomogeneities with the magnetic field inhomogeniety as discussed by Hallatschek and Biskamp[4]. Either mechanism results in GAM zonal flow fluctuations due to nonlinear coupling of driftwave turbulence. Such coupling is shown in the data. An additional interesting result is that the zonal flows were only detected over the normalized radius of $0.65<\rho<0.95$. While zonal flows are predicted to exist at all radii, this is the region with the strongest gradients and strongest driftwave fluctuations which may account for the localized signal. The HIBP measures the potential; the electric field is inferred

Potential fluctuations due to zonal flows have been presented in the past, but were miss-identified. Perhaps, the paper by Tsui et al. shows the clearest example[16]. In this paper fluctuations of potential (from both the HIBP and Langmuir probes) are presented as a quasicoherent mode, resent analysis shows this mode is at the GAM frequency. It was stated that the quasicoherent mode was not related to Mirnov activity, didn't directly cause convective transport of particles, and in another paper the mode was shown to be nonlinearly coupled to driftwave turbulence.[17] The only discrepancy with explaining the results as zonal flow is the statement by Tsui that the Langmuir probes measured a small but finite k_θ, but as noted in that paper the HIBP measured $k_\theta=0$. Other papers have likely presented experimental evidence but failed to identify the zonal flows; for example Hamada[18] presented HIBP data from the JIPP-T2U tokamak.

The remainder of this paper presents reanalyzed HIBP data taken on TEXT. The data is for a discharge with $B_{tor}=2.2T$, $I_p=200kA$, $\bar{n}_e = 2x10^{13}\,cm^{-3}$, $Te(0)\sim880eV$, $Ti(0)\sim550eV$, circular crossection, limited, q(1.0)= 3.3, OH plasma. (Full profiles don't exist for this

discharge, so some of these parameters are estimated using a similar discharge with a slightly stronger toroidal field.) The TEXT HIBP was capable of making fluctuation measurements of potential and density simultaneously at three sample locations. The locations can be scanned across the minor radius during a pulse. Ideally two sample volumes are configured with radial alignment and the electric field is determined by $E_r = -\partial\phi / \partial r$. Unfortunately the data taken didn't have radially aligned sample volumes and the sample volume size was the order of, or likely larger than, the radial correlation length of the zonal flow E_r.

Due to the physics of zonal flows, the HIBP was still able to measure radial electric fields. A flux surface can be looked at as a conducting shell in regards to zonal flows, $E_\theta = 0$ and $E_{||} = 0$, there is only a normal component to the electric field as there would be for a conductor. View the region of a zonal flow as 2 conducting shells and subtract off any dc radial electric field for convenience. If charges are transferred back and forth between these shells, then an electric field oscillation will exist between the shells and nowhere else. This is a zonal flow. If one measures the potential of this system as a function of radius, using the vacuum vessel as a ground reference, there are no potential fluctuations outside of the outer shell (flux surface,) the potential fluctuations vary with radius between the shells, and there will be a spatially uniform potential fluctuation everywhere inside of the inner shell. If the plasma contains multiple zonal flow layers, the measured potential fluctuations at a given location will carry information about all zonal flow layers at radii greater than the sample location. Assuming the flow layers are decorrelated, the interior measurements will be an rms sum of all zonal flow layers. Here

again the physics made the measurement easier, the zonal flows were measured to exist at the GAM frequency, which varies with radius, the frequency changes as the square root of the ion and electron temperatures. Interior measurements are relatively broad in frequency, if subdivided into frequency segments, each segment is the result of flows in a radial range where the GAM matches the measured frequency.

Figure 1 is the spectra of the potential fluctuations at three sample locations made using the 3 detectors of the HIBP on TEXT. These are simultaneous measurements. The sample locations are displaced both poloidally and radially but only the radial displacement matters for zonal flows ($k_\theta=0$). The plot shows that total level of fluctuations changes with radius consistent with the conducting shell model presented in the paragraph above. An interior sample location measures the same fluctuations as a more exterior location, plus additional fluctuations due to flows in the intermediate region.

If one considers the lowest frequency components, 20 – 25 kHz, of the zonal flow fluctuations in Figure 1, one notes that the amplitudes are the same. The conducting shell model states that these are due to zonal flows at radii greater than that of the outer most point, (interior to a conducting shell the potential varies the same everywhere.) Figure 2 reinforces this conclusion by plotting the phase shift vs. frequency for 2 core measurements of potential. The discharge studied has no zonal flows for $\rho<0.65$, so samples interior to this radius measure the sample amplitude and phase everywhere. If

the mode had an m=1 structure, the phase shift would be 0.4 radians in figure 2. Clearly these fluctuations are coherent and in phase.

Figure 3 is the auto power spectrum of a signal created by taking the time domain difference of the potential signal for 2 sample locations $(\phi_1 - \phi_2)$, both of which are in the region where zonal flows exist. If the samples were located close together, the electric field could be estimated by $E_x = -\partial\phi / \partial x \approx (\phi_1 - \phi_2)/(x_2 - x_1)$, where x is in the direction between the sample volumes. For zonal flows there is only a radial component to the electric field, so x can be replaced with r. For this data, the sample volume spacing is greater than the apparent radial correlation length of the zonal flows, so the proper scaling is not $(x_2 - x_1)$ but rather something on the order of the radial correlation length; which is not measured. Figure 3 therefore represents a signal that is proportional to the zonal flow electric fields that exist between the 2 sample locations. It shows that zonal flows, in the region $0.69<\rho<0.76$, occur in the frequency range of 37 to 44 kHz, (full width, half maximum.) Data was taken for various sample locations and orientations using several plasma pulses all with the same discharge condition. All of the sample locations are in the upper outer quadrant of the plasma cross-section. Figure 4 is a plot of this collection. For each point, the horizontal bar represents the radial displacement of the sample locations, the vertical bar represents the range of frequencies in the zonal flow electric fields, (as was shown in figure 3.) Plotted against this data is an estimate of the GAM frequency vs. radius for this discharge condition. There are no temperature profiles for this discharge condition, rather profiles for a similar discharge condition were used. The frequency of the GAM varies as the square root of the temperature, so it is

relatively insensitive to errors in the profiles. As is seen, the zonal flow electric field fluctuations closely match the estimated GAM frequency as a function of radius.

The zonal flows are not directly driven by the free energy stored in the radial gradients. Rather, nonlinear processes, such as the drift wave Reynolds stress[1] or Stringer-Wilsor term[4, 19], couple the drift wave turbulence to the zonal flows. In either case, the best test of the data for nonlinear coupling is to check for 3-wave coupling in the potential fluctuation data.[10] In general, the HIBP does measure broadband driftwave fluctuations and results from TEXT and TEXT-U have been reported.[20,21] These fluctuations

$$b^2(f_1,f_2)=\left\langle \frac{\left|N_e(f_1)N_e(f_2)\Phi^*(f_1+f_2)\right|^2}{\left|N_e(f_1)\right|^2\left|N_e(f_2)\right|^2\left|\Phi(f_1+f_2)\right|^2}\right\rangle \qquad (1)$$

dominate the TEXT spectra for frequencies in the 50 to 300kHz range, and are found to be nearly Boltzmann like $\left(\tilde{n}/n\approx\tilde{\phi}/T_e\right)$ for radii other than near the plasma edge. Unfortunately, the signal to noise of the potential fluctuations presented herein is very poor over most of the driftwave spectral range. By assuming that the driftwave density and potential fluctuations are correlated[20,21], a nonlinear coupling test of the data is done using the density fluctuations cross-correlated with the potential fluctuations. This is a valid test of cross bicoherence but resultant relative phase shifts measured this way are of questionable value. Figure 5 has 3 plots showing the cross bi-coherence, b^2 defined in equation 1 where $N_e(f)$ and $\Phi(f)$ are the fourier transforms of $n_e(t)$ and $\varphi(t)$. Only a selected frequency range is displayed to emphasis the region of interest. The potential fluctuation data is taken at $\rho=0.69$ in all cases. The density data is taken for each of the 3 sample locations ($\rho=0.69,\ 0.76$, and 0.85). It is reasonable to use potential data from a

location interior to the density data because the interior potential data carries information about zonal flows at all larger minor radii. The second plot in figure 5 shows that at rho=0.76, the driftwave fluctuations at frequencies of 150 to 400kHz are coupled to the zonal flows at 40kHz, (the interior potential fluctuation measurement retains information about flow at this outer radius.) The third plot shows that at rho=0.85, the driftwaves are coupled to zonal flows at 20kHz. The frequency resolution of these plots is only 8kHz due to the averaging needed to reduce the noise floor of the cross bi-coherence. Shot-to-shot averaging would allow better resolution.

As stated, the potential and density fluctuations are Boltzmann like for frequencies above the range of the zonal flows. In the zonal flow frequency range of 20 to 50kHz the fluctuations are far from Boltzmann with the normalized potential fluctuations being about 2 orders of magnitude stronger than the normalized density fluctuations (in terms of auto power) and at best there is only a weak linear coupling between the density and potential. Diamond et al. predict that for the zonal flows $\tilde{n}/n \approx \left(k_\perp{}^2/\rho_s{}^2\right)\left(\tilde{\phi}/KT_e\right)$. For TEXT $k_\perp{}^2/\rho_s{}^2$ is estimated to be in the range of 0.01 to 0.1 This puts the measured relative fluctuation level in agreement with this prediction.

The radial mode structure of the zonal flow wasn't measured with this diagnostic because of the relatively large sample volume size and large sample spacing. The structure is important because the potential measurement will underestimate the effective local E_r if the zonal flow correlation length, $l_c(zf)$, is large compared to the zonal flow radial wavelength, $2\pi/k_r(zf)$, where $k_r(zf)$ is the radial wavenumber for the zonal flow. For

$l_c(zf) > \pi/k_r(zf)$, E_r will reverse within a correlation length and the path integrated E_r (the measured ϕ) significantly underestimates the peak local E_r. The conducting shell model presented is the opposite case - a short correlation length compared to the wavelength, and the measured ϕ is an accurate measure of the effective E_r.

As stated above, figure 3 presents fluctuating autopower of a signal that is proportional to the zonal flow radial electric field. The proportionality factor can be estimated using the following assumptions: 1) $l_c(zf) < \pi/k_r(zf)$ 2) Zonal flows exist in multiple layers, each with a thickness of $l_c(zf)$ and 3) $l_c(zf)$ is the order of $5\rho^*$. In this case each zonal flow layer produces a potential fluctuation with $\tilde{\phi} = \tilde{E}_r l_c(zf)$. The resultant $\tilde{E}_r$ for this discharge at rho=0.8 is 30kV/m. This is the same order as the profile E_r, or $\langle E_r \rangle$. It would drive fluctuating flows that have a poloidal velocity of the same order as the electron diamagnetic drift velocity, in other words $v(\langle E_r \rangle) \sim |v(\tilde{E}_r)| \sim v_{de}$. The velocity due to the profile radial electric field is in the electron diamagnetic drift direction. This estimate of the zonal flow velocity is very crude.

The zonal flow radial electric field has been measured in TEXT using an HIBP. Measurements of potential have been shown to be due to a fluctuating E_r with an m=0 mode structure. The HIBP didn't measure the parallel mode structure, but all results are consistent with an n=0. The potential fluctuations are at the GAM frequency, and to the limit of the diagnostic, as configured, there is no measurable f=0Hz component. The zonal flows are found to be in a limited radial range of 0.65<rho<0.95. This is the region of the largest gradients and where the driftwave fluctuations are relatively strong. The

zonal flow fluctuations are nonlinearly coupled to the broadband driftwave turbulence. A crude estimate of the magnitude of the zonal flow E_r results in a flow velocity of the same order as the profile *ExB* and v_{de} velocities.

The author wishes to thank the Fusion Research Center at UT-Austin (Ron Bravenec and Don Patterson in particular,) for retrieving old data and profiles. This work could not have been done in the US if not for the TEXT and TEXT-U data set. I also need to thank Stewart Zweben for suggesting that we look for zonal flow characteristics in the HIBP data, and thank T.S. Halm and Bruce Scott for discussions, comments and encouragement.

Figure Captions:

Figure 1 Auto power spectra for fluctuations of potential at three sample locations. Interior potential fluctuations are due to all zonal flow fluctuations at larger radii, so total fluctuation level increases as the sample location is moved inward.

Figure 2 a) Auto power spectra for 2 interior points showing equal power at both sample locations. Circles are for rho=0.40, theta=8^o X are for rho=0.35 and theta=31. b) Coherence vs. frequency and c) Relative phase vs. frequency. The 0^o phase shift demonstrates the mode is m=0.

Figure 3 Auto power spectra of potential (at 2 locations,) and the difference spectra, $F(\Delta\varphi)$. The difference spectra is the result of zonal flows in the region $0.69<\rho<0.76$

Figure 4 Frequency of zonal flow E_r vs. radius, plotted with the GAM frequency estimate (line with no symbols.) Vertical lines on data points show frequency range for fluctuations of E_r from one pair of sample locations. Horizontal lines show radial spacing of samples.

Figure 5 Cross bicoherence for 3 selections of data. Shows nonlinear coupling between the broadband driftwave fluctuations and the zonal flow fluctuations of potential. In all cases the potential signal at $\rho=0.69$ is cross correlated with the density fluctuations as described by equation 1. In plot a) the density fluctuations are from the same location as the potential fluctuations, $\rho=0.69$ and the cross bicoherence is significant at frequencies near 50kHz. For plot b) the density fluctuations are for $\rho=0.76$ and the cross bicoherence

is significant near 40kHz For plot c) the density fluctuations are for ρ=0.85 and the coupling is at about 20Hz. Only a portion of the frequency space is plotted to highlight the region of interest.

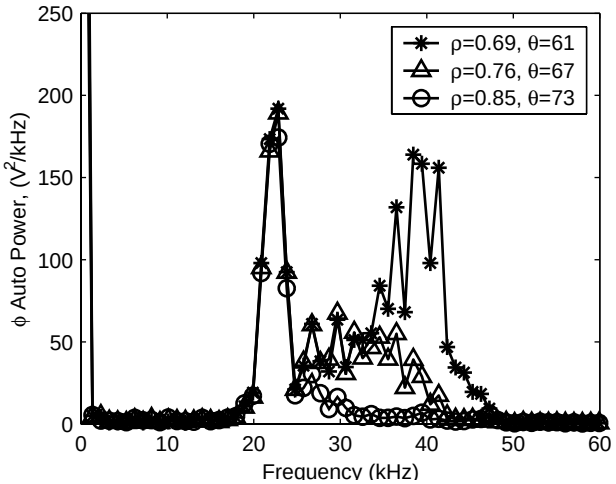

Figure 1 Schoch Phys. Rev. Lett.

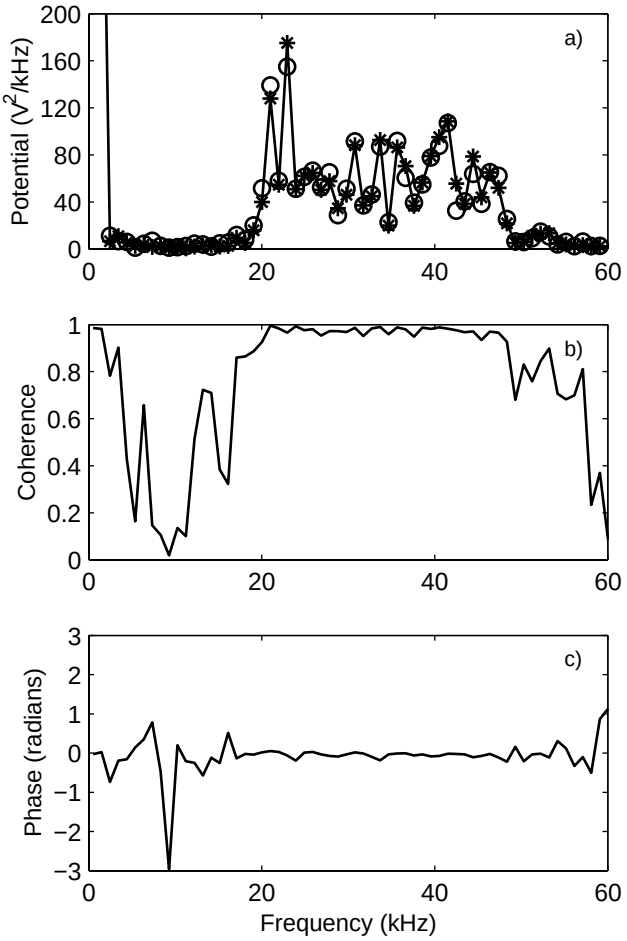

Figure 2 Schoch Phys. Rev. Lett.

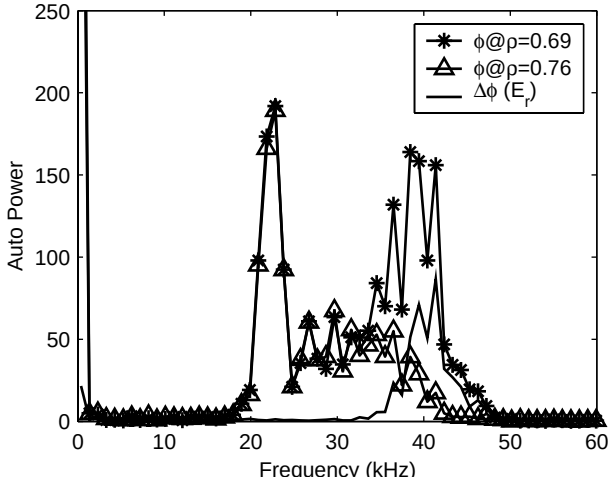

Figure 3 Schoch Phys. Rev. Lett.

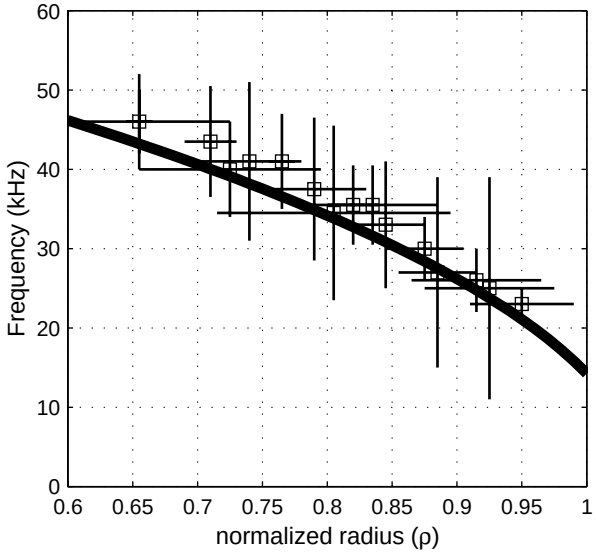

Figure 4 Schoch Phys. Rev. Lett.

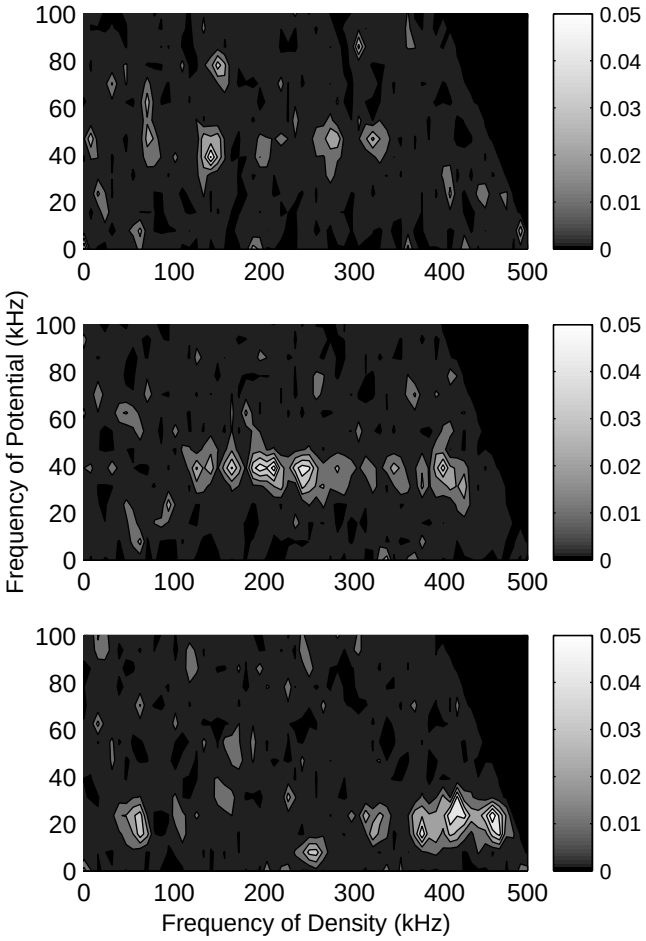

Figure 5 Schoch Phys. Rev. Lett.

References:

[1] P.H. Diamond et al., in Proceedings of the 17th IAEA Fusion Energy Conference, Yokohama, (1998).

[2] K. Itoh et al., Plasma Phys. Controlled fusion **38**, 1 (1996).

[3] P.W. Terry, Rev. Mod. Phys. **72**, 109 (2000).

[4] K. Hallatschek, et al., Phys. Rev. Lett. **86**, 7 p. 1223 (2001).

[5] T.S. Hahm, et al., Plasma Phys. Control. Fusion **43** p. A205 (2000).

[6] M.G. Shats, Phys. Rev. Lett. **88**, 045001 (2002).

[7] S. Coda, et al., Phys. Rev. Lett., **86**, (21) p. 4835, (2000).

[8] M. Jakubowski et al., Bull. Amer. Phys. Soc. **46**, 8 p. 221 (2001).

[9] G.R. Tynan et al., Phys. Plasmas **8**, 2691 (2001).

[10] R.A. Moyer et al., Phys. Rev. Lett. **87**, 135001 (2001).

[11] T.P. Crowley et al., IEEE Trans. Plasma Sci., **22**, 4 (1994).

[12] K.W. Gentle Nuclear Technology/Fusion **1**, 4, p. 479 (1981).

[13] N. Winson et al., Phys. Fluids **11**, (11) p. 2448 (1968).

[14] L. Th. M. Ornstein and K.M. Young Bull. Am. Phys. Soc. **13**, 286 (1968).

[15] Conversation with Dr. Kenneth M. Young, PPPL, (2002).

[16] H.Y.W. Tsui, et al., Phys. Fluids B **5** (4) p. 1274 (1993).

[17] H.Y.W. Tsui, et al., Phys. Rev. Lett, **70** (17) p. 2565 (1993).

[18] Y. Hamada, et al., Fusion Eng. Des. **34-35**, p. 663 (1997).

[19] A.B. Hassam et al., Phys. Plasma **1**, 337 (1994).

[20] J.C. Forster et al., IEEE Trans. on Plasma Sci. 22 (4) p. 359 (1994).

[21] Demers et al., Phys. Plasma **8**, 1278 (2001).